J Neurophysiol 94: 1837–1848, 2005;
doi:10.1152/jn.00260.2005.

Interaction Between Amygdala and Neocortical Inputs in the Perirhinal Cortex

Joe Guillaume Pelletier, John Apergis-Schoute, and Denis Paré
Center for Molecular and Behavioral Neuroscience, Rutgers, The State University of New Jersey, Newark, New Jersey

Submitted 10 March 2005; accepted in final form 16 May 2005

Pelletier, Joe Guillaume, John Apergis-Schoute, and Denis Paré. Interaction between amygdala and neocortical inputs in the perirhinal cortex. *J Neurophysiol* 94: 1837–1848, 2005; doi:10.1152/jn.00260.2005. The rhinal cortices play a critical role in high-order perceptual/mnemonic functions and constitute the main route for impulse traffic to and from the hippocampus. However, previous work has revealed that neocortical stimuli that activate a large proportion of perirhinal neurons are unable to discharge entorhinal cells. In search of mechanisms that might facilitate impulse transfer from the neocortex to the entorhinal cortex, we have examined changes in excitability produced by activation of the lateral amygdala (LA) in isoflurane-anesthetized animals. LA stimulation activated a large proportion of peri- and entorhinal neurons. However, conditioning LA stimuli did not increase the ability of neocortical inputs to activate entorhinal cells even though such pairing produced marked increases in neocortically evoked field potentials and orthodromic firing in the perirhinal cortex. Moreover, increased neocortically evoked perirhinal field potentials and unit responses persisted when the conditioning LA shock was replaced by another neocortical stimulus at the same or at a different site as the testing shock. This perirhinal paired-pulse facilitation (PPF) was maximal with interstimulus intervals of ~100 ms. Intracellular recordings of perirhinal neurons revealed that the PPF was generally associated with a rapid shift in the balance between inhibition and excitation, leading to an overall increase in perirhinal responsiveness. The significance of these findings for the role of the perirhinal cortex is discussed.

INTRODUCTION

Lesion studies indicate that the rhinal cortices and amygdala contribute to distinct forms of memory. Rhinal lesions interfere with recognition and associative memory (reviewed in Suzuki 1996), whereas amygdala lesions have little effect on tests probing these functions (Parker and Gaffan 1998; Zola-Morgan et al. 1989, 1991). Rather amygdala lesions prevent the development of classically conditioned fear responses (Davis et al. 1994; Kapp et al. 1992; LeDoux 2000). Although such data suggest that the amygdala and rhinal cortices can function independently, other observations indicate that the amygdala influences the rhinal cortices in some conditions. For instance, long-term declarative memory for emotionally arousing material is better than for neutral events, and this effect is absent in subjects with amygdala lesions (Adolphs et al. 1997; Cahill et al. 1995; Richardson et al. 2004). Moreover, several functional imaging studies have reported a high correlation between the amount of amygdala activation at encoding and subsequent recall (Cahill et al. 1996; Hamann et al. 1999).

At present, the mechanisms underlying these effects remain unclear. It is believed that declarative memory formation is achieved through the transfer of highly processed sensory information from associative neocortical areas to the hippocampus (Buzsáki 1989; Pennartz et al. 2002) via a multisynaptic pathway in the superficial layers of the rhinal cortices (Insausti 1987; Room and Groenewegen 1986a; Van Hoesen and Pandya 1975). However, there is a discrepancy between anatomical and physiological data about the rhinal network. Tracing studies indicate that the perirhinal cortex forms strong reciprocal connections with the neo- and entorhinal cortex (reviewed in Witter et al. 2000). In contrast, physiological studies indicate that perirhinal transmission of neocortical and entorhinal inputs occurs with an extremely low probability (Biella et al. 2001, 2003; De Curtis et al. 1999; Pelletier et al. 2004). Thus the amygdala might facilitate declarative memory by enhancing the ability of the rhinal cortices to relay neocortical inputs to the hippocampal formation.

Consistent with this possibility, imaging with voltage-sensitive dyes in vitro has revealed that amygdala stimulation can facilitate the transfer of neocortical inputs to the rhinal cortices and dentate gyrus under conditions of partial $GABA_A$ blockade (Kajiwara et al. 2003). Moreover, the amygdala sends powerful projections to the rhinal cortices. Most amygdala projections to the rhinal cortices originate in the basolateral amygdaloid complex (BLA), which includes the lateral (LA), basolateral, and basomedial nuclei (Krettek and Price 1977a,b; Room and Groenewegen 1986b; Smith and Paré 1994; reviewed in Pitkänen 2000). Ultrastructural studies have revealed that BLA axon terminals are enriched in glutamate and form asymmetric synapses, typically with dendritic spines on their cortical targets (Paré et al. 1995; Smith and Paré 1994). The LA contributes a particularly massive projection to both the peri- and entorhinal cortices. Although LA axon terminals are widely distributed across rhinal layers in cats, they are most concentrated superficially (Krettek and Price 1977a,b; Room and Groenewegen 1986b; Smith and Paré 1994). Because superficial rhinal layers also receive inputs from laterally adjacent associative neocortical areas (Room and Groenewegen 1986a), LA and neocortical inputs can potentially converge on the same rhinal neurons.

Thus the present study was undertaken to examine how amygdala inputs affect the responsiveness of rhinal neurons to neocortical inputs using multiple simultaneous extracellular recordings of peri- and entorhinal neurons as well as intracellular recordings under isoflurane anesthesia. Although our

Address for reprint requests and other correspondence: D. Paré, CMBN, Aidekman Research Center, Rutgers, The State University of New Jersey, 197 University Ave., Newark, NJ 07102 (E-mail: pare@axon.rutgers.edu).

The costs of publication of this article were defrayed in part by the payment of page charges. The article must therefore be hereby marked "*advertisement*" in accordance with 18 U.S.C. Section 1734 solely to indicate this fact.

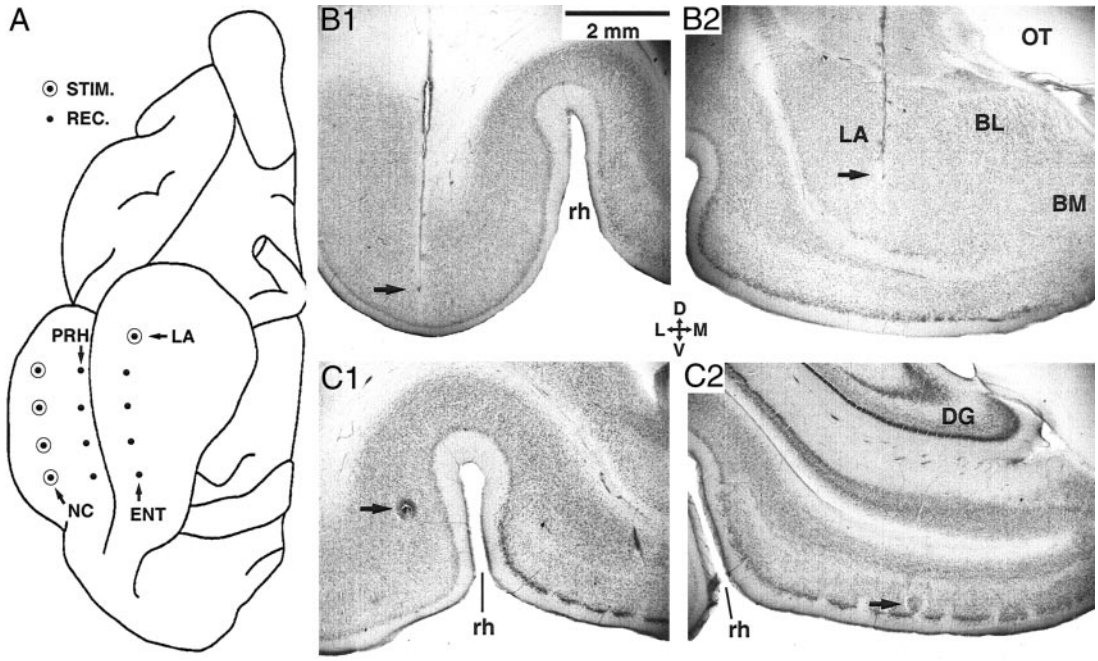

FIG. 1. Experimental setup and histological verification of recording sites. *A*: scheme of the ventral aspect of the cat brain showing the position of recording electrodes (REC, ●) in the perirhinal (PRH) and entorhinal (ENT) cortices as well as the location of stimulating electrodes (STIM., ⊙) in the temporal neocortex (NC) and lateral nucleus of the amygdala (LA). *B*: histological verification of stimulating sites in the temporal neocortex (*B1*) and LA (*B2*). *C*: histological verification of recording sites in the perirhinal (*C1*) and entorhinal (*C2*) cortex. → in *C,* the position of electrolytic lesions made at the end of the experiments to mark the position of interesting neurons recorded previously. DG, dentate gyrus; BL, basolateral nucleus; BM, basomedial nucleus; H, hippocampus; OT, optic tract; rh, rhinal sulcus.

results indicate that amygdala inputs can facilitate the responsiveness of perirhinal cells to neocortical inputs, they also suggest that paired neocortical stimuli are equally effective in this respect. In addition, despite the facilitated response of perirhinal neurons to neocortical stimuli, entorhinal cells remained unresponsive to neocortical stimuli.

METHODS

All procedures were approved by the Institutional Animal Care and Use Committee of Rutgers State University, in compliance with the Guide for the Care and Use of Laboratory Animals (Department of Health and Human Services). Twenty-two adult male cats (2.5–3.5 kg) were preanesthetized with a mixture of ketamine and xylazine (15 and 2 mg/kg im) and artificially ventilated with a mixture of ambient air, oxygen, and isoflurane. Atropine (0.05 mg/kg im) was administered to prevent secretions. The end-tidal CO_2 concentration was maintained at 3.7 ± 0.2%, and the body temperature at 37–38°C using a heating pad. The level of anesthesia was assessed by continuously monitoring the electroencephalogram and electrocardiogram. The bone overlying the amygdala and rhinal cortices was removed and the dura mater opened.

Extracellular experiments

To activate neocortical inputs to the rhinal cortices, four concentric stimulating electrodes were inserted in the temporal neocortex immediately lateral to perirhinal area 36 (Fig. 1, *A,* ⊙, and *B1*). A concentric stimulating electrode was also placed in the lateral nucleus of the amygdala (LA), one of the main sources of amygdala projections to the rhinal cortices (Krettek and Price 1977a,b; Room and Groenewegen 1986b; Smith and Paré 1994; reviewed in Pitkänen et al. 2000) (Fig. 1, *A,* ⊙ marked LA, and *B2,* →).

To record field potentials and unit activity, an array of eight tungsten microelectrodes was stereotaxically aimed at various rostrocaudal levels of the peri- and entorhinal cortex (Fig. 1, *A,* ●, and *C,* →). Microelectrodes were lowered as a group in steps of 5 μm by a micromanipulator (Kopf, Tujunga, CA). Spontaneous and evoked activity was recorded every 100 μm. At the end of each experiment, small electrolytic lesions (0.5 mA for 5 s) were made at locations where neurons of interest were recorded to facilitate histological reconstruction of microelectrode tracks. Animals were then given an overdose of pentobarbital (50 mg/kg iv) and were perfused with 500 ml ice-cold saline (0.9%) followed by 800 ml of a fixative containing paraformaldehyde (2%) and glutaraldehyde (1%) in 0.1 M phosphate buffer (pH 7.4). The brain was then removed and sectioned at 100 μm on a vibrating microtome. Sections were mounted on gelatin-coated slides, air-dried, stained with neutral red, and cover-slipped in Permount for histological verification of electrode placement. Figure 1 shows examples of histologically identified stimulating (*B*) and recording (*C*) sites.

Intracellular experiments

These experiments were conducted on a subset of 12 cats. With the following exceptions, all aspects of the surgery were identical to the approach used for extracellular recordings. To ensure recording stability, the cisterna magna was drained, the hips suspended, and a bilateral pneumothorax was performed. Glass capillary tubing was pulled to a fine tip (≈0.5 μm; ≈40–60 MΩ) and filled with K-acetate (4 M; pH 7.4) and neurobiotin (1%). The perirhinal cortex was approached laterally to minimize travel distance. To this end, the bone overlying the posterior ectosylvian gyrus was removed between frontal planes anterior 5–12 mm. The micropiette penetrated the brain at a depth of +2 to –2 mm, with an angle of 45°. With this approach, the micropipette had to course through 3–6 mm of cortex and white matter to reach the deep layers of the perirhinal cortex. Recordings were made using a high-impedance amplifier with an active bridge circuitry. Typically, cells were recorded for 30–100 min. Bridge balance was checked regularly during the recordings.

After perfusion (see preceding text), the brains were sectioned at 100 μm and processed to reveal neurobiotin. Sections were washed several times in phosphate buffer saline (PBS, 0.1 M, pH 7.4) and then transferred to a sodium borohydride solution (1%) in PBS for 20 min. After numerous washes in PBS, sections were incubated for 12 h at 22°C in a solution containing 1% bovine serum albumin (BSA), 0.3% triton, 1% solutions A and B of an ABC kit (Vector, Burlingame, CA) in PBS. The next day, they were washed in PBS (2 × 10 min) and immersed in a Tris buffer (0.05 M, pH 7.6; 10 min). Neurobiotin was visualized by incubating the sections in a Tris buffer containing 10 mM imidazole, 700 μM diaminobenzidine and 0.3% H_2O_2 for 8–10 min. Then the sections were washed in PBS (6 × 5 min), mounted on gelatin coated slides, air dried, dehydrated in a graded series of alcohol, and coverslipped with permount for later reconstruction.

Analysis

All data were digitized (Vision, Nicolet, Middleton, WI) at 20 kHz and stored on a hard disk. Analysis was performed off-line using IGOR (Wavemetrics, Lake Oswego, OR) and custom-designed software running on Macintosh computers. Histological reconstructions were performed by taking serial pictures at different focal planes and of different sections using a digital camera mounted on a microscope. The images were then manually layered with Photoshop.

RESULTS

Extracellular recordings

DATABASE. A total of 584 perirhinal and 586 entorhinal neurons were recorded extracellularly in this study. Electrical stimulation of the LA produced orthodromic activation in 24.5% of perirhinal and 18.0% of entorhinal neurons recorded at rostral levels (2 rostral-most electrode rows in Fig. 1*A*, n = 271 and 284, respectively). Consistent with the fact that the LA projects less intensely to the caudal portion of the rhinal cortices (Krettek and Price 1977a,b; Room and Groenewegen 1986b; Smith and Paré 1994; reviewed in Pitkänen et al. 2000), the proportion of responsive cells was significantly lower caudally (12.0 and 8.1% of peri- and entorhinal neurons, respectively; 2 caudal-most electrode rows in Fig. 1; n = 313 and 302, respectively; χ^2, $P < 0.05$).

Figure 2 depicts examples of orthodromically activated perirhinal (*A1*) and entorhinal (*B1*) neurons as well as post-stimulus histograms of evoked unit activity (*A2* and *B2,* respectively). Orthodromic activation latencies ranged usually between 7 and 30 ms in both structures (average 17.9 ± 0.8 and 18.4 ± 0.8 ms for peri- and entorhinal neurons; *A3* and *B3,* respectively). Consistent with previous findings (Pelletier and Paré 2002), orthodromic response latencies did not vary as a function of the rostrocaudal position of recorded cells (*t*-test, $P > 0.05$).

EFFECT OF CONDITIONING LA STIMULI. The effectiveness of LA stimuli in activating neurons on both sides of the rhinal sulcus contrasts with the asymmetric distribution of rhinal neurons responsive to neocortical stimuli (Pelletier et al. 2004). Indeed, in this recent study, it was reported that electrical stimuli delivered in the temporal neocortex orthodromically activated 39 and 1.4% of peri- and entorhinal cells, respectively.

To investigate whether amygdala inputs can facilitate the transfer of neocortical volleys to the entorhinal cortex, we compared the responsiveness of peri- and entorhinal neurons to testing neocortical shocks, applied in isolation or preceded by

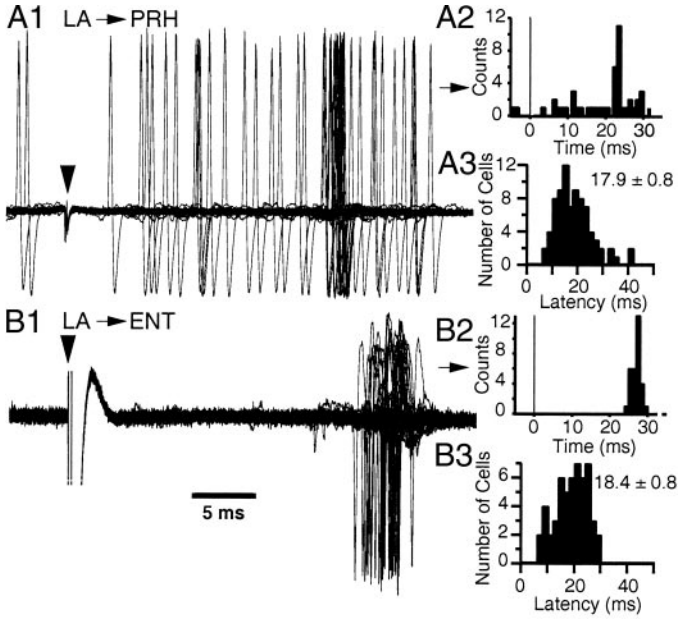

FIG. 2. Orthodromic activation of perirhinal (*A*) and entorhinal (*B*) neurons following stimulation of the lateral amygdala. In *A* and *B*, *1* shows superimposed sweeps where the LA stimulation artifact is marked by an arrowhead. *Panel 2* shows a peristimulus histogram for the same cell as in *1*. *Panel 3*, shows the frequency distribution of response latencies across our sample.

conditioning LA stimuli. Initially, we focused on field responses recorded in superficial layers because tract-tracing studies have revealed that LA and neocortical projections mainly target superficial rhinal layers I–III (Insausti 1987; Room and Groenewegen 1986a; Smith and Paré 1994). Neocortical stimulation elicited field responses in both perirhinal (Fig. 3*A1*) and entorhinal (*A2*) cortices. The *inset* in Fig. 3*B2* indicates how the amplitude of these field potentials was measured. Preceding the neocortical stimulus by a conditioning LA shock with interstimulus intervals (ISIs) ranging between 70 and 200 ms enhanced amplitude of neocortically evoked field potentials in the perirhinal (Fig. 3*A1*) and entorhinal (*A2*) cortices. This effect was maximal at an ISI of ~100 ms in the perirhinal cortex (Fig. 3*B*) and the entorhinal cortex. With this ISI, conditioning LA shocks increased neocortically evoked field potentials by 163.7 ± 22.17 and 164.7 ± 13.8% of baseline in the peri- and entorhinal cortices, respectively (*t*-test $P < 0.05$, n = 10; Fig. 3*A3,* bars marked L).

EFFECT OF PAIRED NEOCORTICAL STIMULI. To investigate whether this effect was a unique property of LA inputs, we tested whether paired neocortical stimuli would have the same effect. Because the facilitation produced by conditioning LA stimuli depended on the ISI (Fig. 3*B2*), an interval scan was performed for paired neocortical stimuli as well (n = 10). As shown in the example of Fig. 3*C*, maximal increases in the amplitude of neocortical-evoked field potentials in the perirhinal cortex occurred at an ISI of ~100 ms. This ISI was therefore used for all experiments described in the following text. With this ISI, the increases in neocortically-evoked field potentials averaged 162.1 ± 14.1 and 173.4 ± 14.5 of baseline in the peri- and entorhinal cortex, respectively (Fig. 3*A3,* bars marked C). On average, the magnitude of the potentiation seen with LA and neocortical conditioning stimuli was not statistically different (paired-*t*-test, $P > 0.05$).

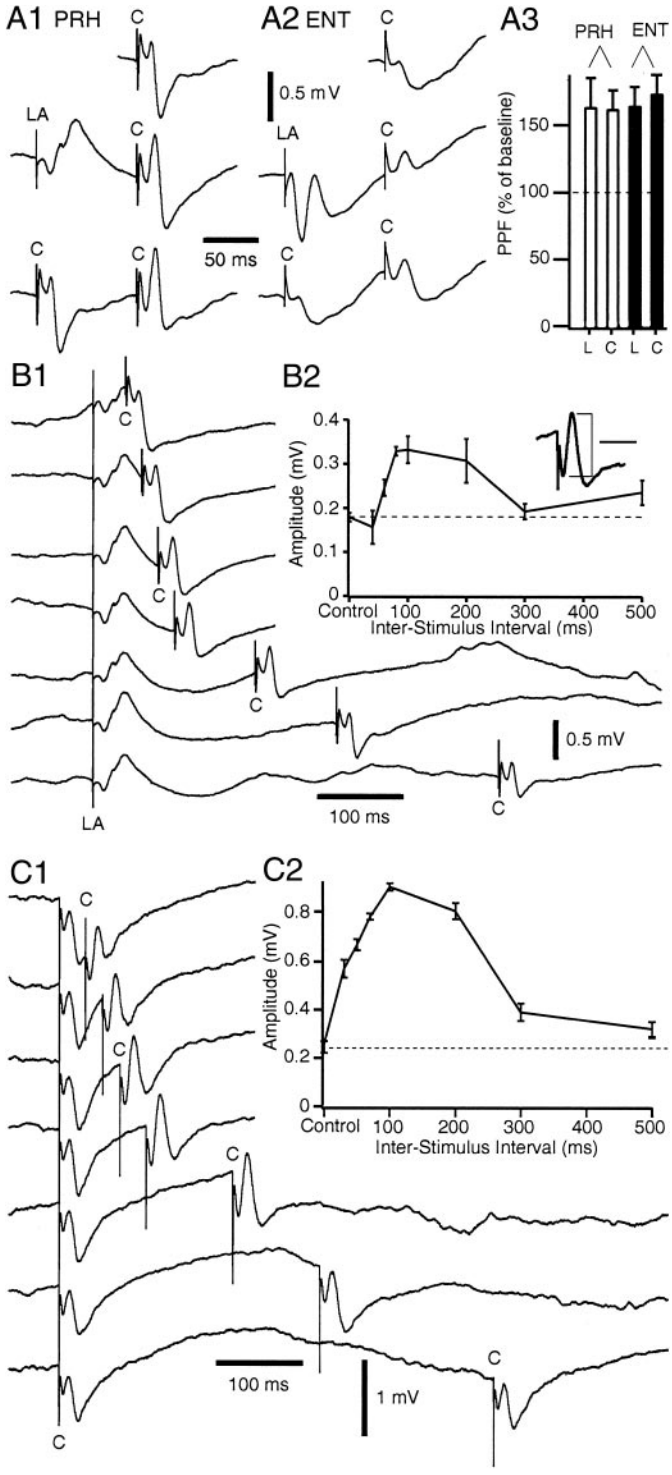

FIG. 3. Facilitation of neocortically evoked field responses by conditioning LA and neocortical stimuli in the perirhinal (*A1, B,* and *C*) and entorhinal cortices (*A2*). *A*: field responses evoked by stimulation of the temporal neocortex (*top*) in the perirhinal (*A1*) and entorhinal (*A2*) cortices are potentiated when preceded by conditioning LA (*middle*) or neocortical (*bottom*) stimuli. *A3*: amount of paired-pulse facilitation (PPF) seen in the perirhinal (□) and entorhinal (■) cortices with LA (marked L) and neocortical (marked C) conditioning stimuli (averages of 10 experiments). *B* and *C*: recording in the perirhinal cortex, using various intervals between the conditioning and testing shocks, reveals that for both LA (*B*) and neocortical (*C*) stimuli, the interstimulus interval (ISI) causing the most PPF is ~100 ms.

EFFECT OF PAIRED STIMULI ON UNIT RESPONSIVENESS. We then sought to determine whether the changes in neocortically evoked field potentials produced by paired stimuli were associated to modifications in the responsiveness of peri- and entorhinal neurons, as previously seen in other structures (Leung and Fu 1994; Marder and Buonomano 2003). To this end, the data were filtered (0.3–20 kHz) and unit responsiveness to single or paired LA and neocortical stimuli were compared. Responsiveness was operationally defined as the number of evoked spikes divided by number of stimuli. The stimulation intensity was adjusted so that single shocks orthodromically activated the tested cells in ~20–30% of trials.

In 33 of 46 tested perirhinal neurons (or 72%), conditioning LA stimuli enhanced orthodromic responsiveness to neocortical stimuli (342 ± 65% of baseline). In the remaining cells ($n = 13$), the responsiveness to the second shock was reduced ($n = 12$) or unchanged ($n = 1$). An example of the increased unit responsiveness produced by LA conditioning shocks is shown in Fig. 4*A*. Note that LA conditioning shocks not only increased the number of orthodromic responses (Fig. 4*A*) but also of antidromic invasions (Fig. 4*B*). The latter phenomenon was seen in all cells whose antidromic responses occurred with a low probability ($n = 7$, Fig. 4*B*). Here, it should be noted that the latency of antidromic perirhinal responses to LA stimuli depicted in Fig. 4*B* is within the range previously reported for this pathway (Pelletier et al. 2002). Similarly, paired neocortical stimuli increased the orthodromic responsiveness of most perirhinal cells (28 of 38 tested cells (or 74%); average: 306 ± 100% of baseline; Fig. 4*C*).

In contrast, the responsiveness of entorhinal neurons to neocortical stimuli was unchanged by conditioning LA shocks. That is, unresponsive entorhinal cells remained so when a conditioning LA shock was applied before neocortical stimuli (64 of 64 tested cells). Figure 5*A* shows examples of entorhinal neurons that remained unresponsive to neocortical stimuli even when the testing shocks were preceded by conditioning LA stimuli. Similarly, paired neocortical stimuli failed to enhance the orthodromic responsiveness of all tested entorhinal neurons ($n = 59$): that is, most entorhinal neurons were unresponsive to neocortical stimuli and remained so even when paired stimuli were applied. In fact, Fig. 5*B* shows the only case in our sample of entorhinal neurons that could be orthodromically activated by neocortical stimuli. Yet, the responsiveness of this cell to the second shock was reduced. These results suggest that the increased magnitude of neocortically evoked field potentials seen in the entorhinal cortex after conditioning LA or neocortical stimuli was volume conducted from the perirhinal cortex or that the increased excitatory drive suggested by the field potential was insufficient to overcome the local inhibition.

Finally, increases in perirhinal (22 of 27 or 81%; Fig. 5*C*) and entorhinal (11 of 16 or 69%; Fig. 5*D*) unit responsiveness were also seen with paired LA stimuli. In these cells, the responsiveness to the second shock averaged 298 ± 100 and 264 ± 30% of baseline, respectively.

Although this phenomenon was not investigated in detail, we routinely observed that the facilitation of orthodromic responsiveness produced by paired stimuli could be transformed into a depression when the stimulation intensity was increased such that the first LA shock elicited orthodromic spikes in most trials. Yet even in such cases, field responses

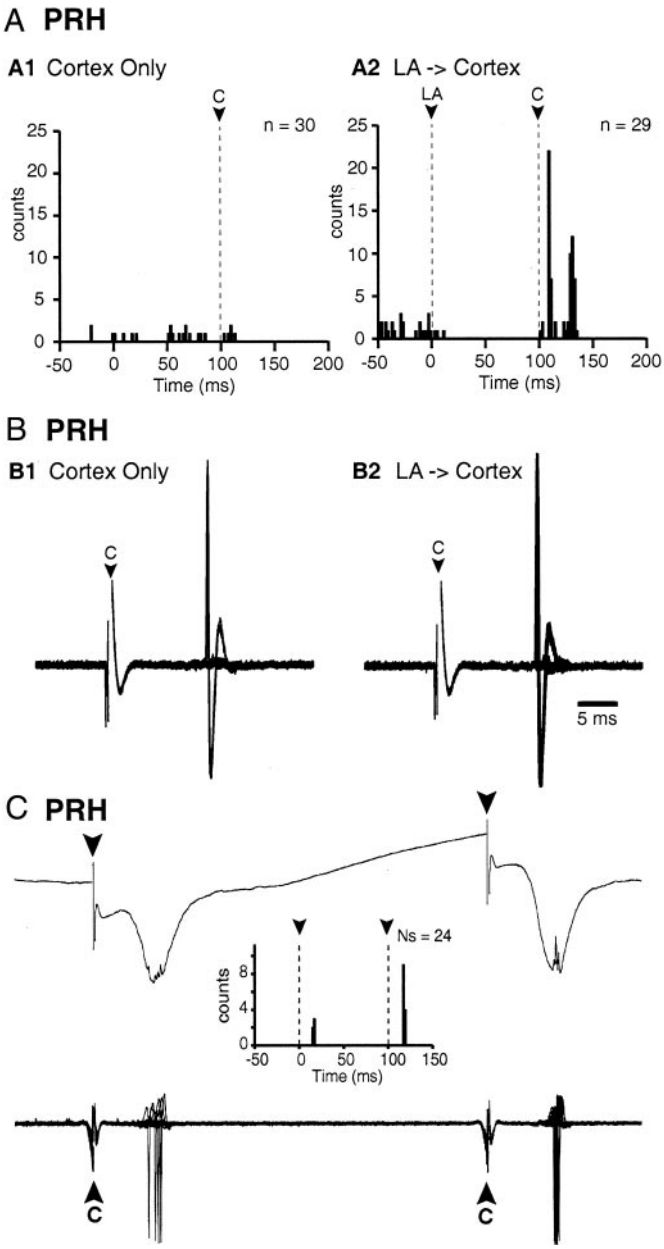

FIG. 4. Conditioning LA stimuli produce a facilitation of neocortically evoked orthodromic (*A*) and antidromic (*B*) responses in the perirhinal cortex. *A*: peristimulus histograms of perirhinal discharges around a neocortical stimulus delivered alone (*A1*) or preceded by a conditioning LA shock (*A2*). *B*: superimposed sweeps showing antidromic response of a perirhinal neuron to neocortical stimuli delivered in isolation (*B1*) or preceded by conditioning LA shocks (*B2*). The probability of antidromic invasion increased from 20% in *B1* to 60% in *B2*. *C*: paired neocortical stimuli produce a facilitation of orthodromic responses in a perirhinal neuron. *Top* and *bottom,* respectively, show the field potential and unit responses (superimposed sweeps) recorded simultaneously by the same microelectrode after differential digital filtering (field, 0.1–300 Hz; unit, 0.3–20 kHz). *Inset*: a peristimulus histogram for the same cell.

recorded by the same microelectrode continued to display paired-pulse facilitation (PPF). This phenomenon was also observed with paired neocortical stimuli.

In vivo intracellular recordings of perirhinal neurons

DATABASE. To examine the mechanisms underlying the PPF observed in extracellular experiments, intracellular recordings of perirhinal neurons were performed. In addition to potassium acetate (4 M), the pipette solution contained neurobiotin (1%) to allow morphological identification of recorded cells. Although we generally recorded more than one neuron per track, as a rule we only recovered the last recorded cell. To be included in our sample, neurons had to meet the following criteria: they had to have a stable resting membrane potential equal or negative to −60 mV and generate overshooting action potentials in response to depolarizing current injection. Recorded cells could be formally identified as perirhinal neurons, either because they were visualized post hoc ($n = 14$), or were recorded in the same electrode track as a recovered neuron ($n = 17$).

A total of 31 perirhinal cells met these criteria. They were distributed uniformly in the deep (layers V–VI, $n = 16$) and superficial (layers II–III, $n = 15$) layers of the perirhinal cortex. Figure 6 shows three representative examples of neurobiotin-filled perirhinal neurons (Fig. 6, *A, C,* and *D*) and their respective locations (Fig. 6*B*). All recovered cells were pyramidal-shaped, had spiny dendrites extending up to layer I (Fig. 6, *A, C,* and *D1*) and had a highly collateralized axon that bore varicosities (Fig. 6*D2*).

Because this is the first in vivo intracellular study of perirhinal neurons, we first describe their spontaneous and current-evoked behavior. Perirhinal cells had an average resting potential of −77.8 ± 1.4 mV and an input resistance of 29.4 ± 1.3 MΩ and generated overshooting action potentials (66.3 ± 0.5 mV) in response to depolarizing current injection from rest. Consistent with the low spontaneous firing rates seen in extracellular recordings (Pelletier et al. 2004), most intracellularly recorded perirhinal cells (77%) were silent at rest and displayed slow membrane potential oscillations at 0.5–1 Hz (Fig. 7*A, bottom*) that paralleled field potential oscillations recorded in the vicinity (Fig. 7*A, top*). In the few spontaneously firing perirhinal cells we recorded (23%), spikes usually occurred during the depolarizing phase of slow membrane potential oscillations (Figs. 7*B1* and 8, *A* and *B*).

In terms of electroresponsive behavior, all but three of the cells generated spike trains that displayed frequency accommodation in response to supra-threshold current injection (Fig. 7*B3*), similar to the ubiquitous regular spiking cells that were previously described in neocortex (Connors et al. 1982). The rest of our sample ($n = 3$) consisted of bursting neurons reminiscent of the intrinsically bursting cells found in neocortex (Fig. 8). At rest, these cells had a particularly striking pattern of spontaneous activity consisting of high-frequency (≤150 Hz) spike bursts that recurred at a frequency of ≤5 Hz (Fig. 8). We did not attempt to study PPF in these cells because they were too few in numbers and they showed a markedly nonlinear behavior.

INTRACELLULAR ANALYSIS OF PPF IN PERIRHINAL NEURONS. To examine this point, we used stimulation intensities that evoked subthreshold responses in ≥30% of trials at depolarized levels of around −60 mV. This approach was used to avoid contamination of postsynaptic potentials (PSPs) by action potentials and afterhyperpolarizations. Responses were examined in a range of membrane potentials as determined by intracellular current injection. To reproduce the conditions of the extracellular experiments, we also tested stimulus intensities where the first shock evoked spikes in 20–30% of trials at rest.

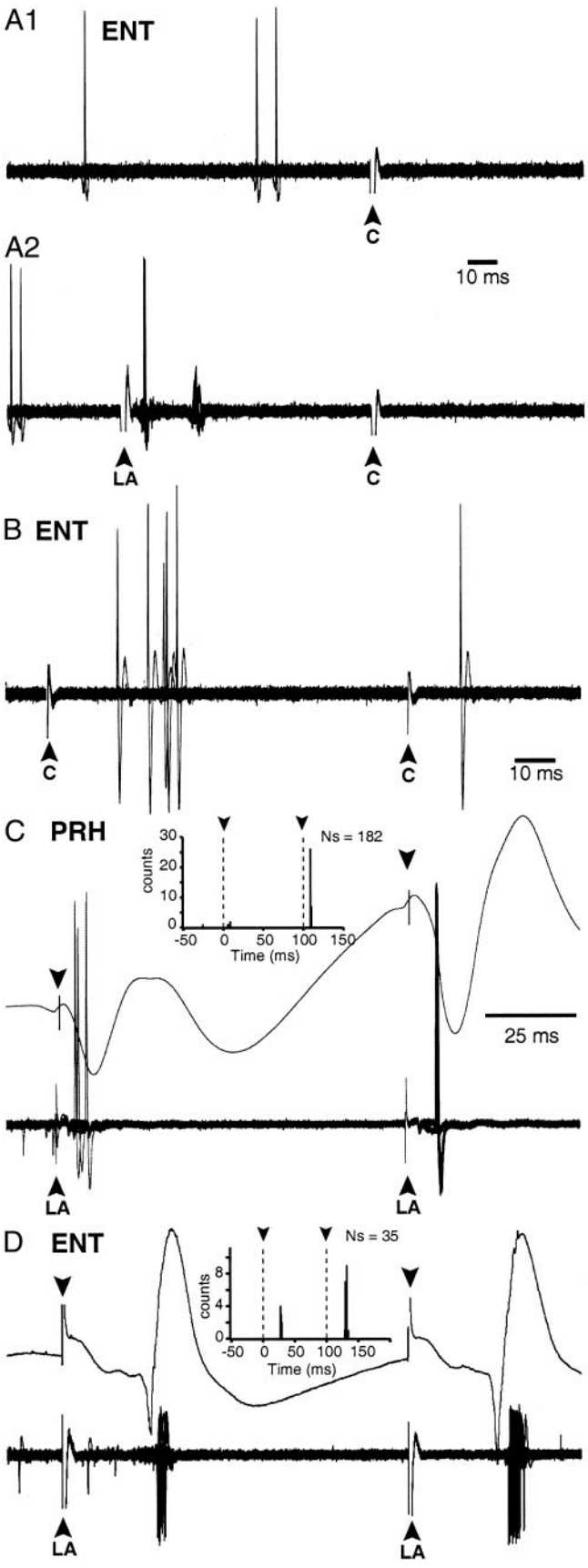

Although the amplitude and pattern of evoked responses varied from cell to cell, all recorded neurons responded similarly to LA and neocortical stimuli. Three major patterns of responses to neocortical and LA stimuli were observed. The first two were seen in cells that displayed PPF. The last one was associated with PPD. These three cell groups are described in turn below. Note that the incidence of these three response patterns did not vary as a function of the depth of the recorded cells.

GROUP 1: perirhinal neurons showing predominantly inhibitory responses and PPF. In close to half our sample (12 of 28 or 43%), both LA and neocortical stimuli evoked monophasic inhibitory PSPs (IPSPs) that were preceded by low-amplitude EPSPs (Fig. 9*A*). From −60 mV, IPSPs evoked by LA or neocortical stimuli had a peak amplitude of –7.6 ± 1.7 and –7.4 ± 1.3 mV and a reversal potential of –71.2 ± 3.4 and –73.6 ± 2.7 mV, respectively. Because the response patterns of these cells to LA and neocortical stimuli were indistinguishable (paired *t*-test, $P > 0.05$), in the remainder of this section, the results obtained with these two stimulation sites will be pooled for simplicity.

In these group I neurons, repetitive stimulation of the LA or neocortex (2–3 shocks at 10 Hz), produced a progressive increase in EPSP amplitude (arrowheads in Fig. 9*A2*), accompanied by a decrease in IPSP amplitude. From the first to the third shock, the shift in excitatory PSP (EPSP) and IPSP amplitude averaged 3.9 ± 0.7 and –5.8 ± 0.9 mV, respectively. Analysis of the responses at different membrane potentials revealed that the initial EPSPs had an extrapolated reversal potential of –38.3 ± 4.3 mV, suggesting that they were contaminated by feed-forward inhibition. Accordingly, the term EPSP will be used with quotation marks in the rest of this section. The shifts in PSP amplitudes were paralleled by modifications of their reversal potentials (Fig. 9, *B1,* IPSP, and *C1,*"EPSP"). Indeed, the extrapolated reversal potential of the "EPSP" shifted positively, on average 28.1 ± 9.2 mV from the first to the second shock (*t*-test, $P < 0.05$). Similarly, the IPSP reversal potential shifted positively by 6.8 ± 1.2 mV from the first to the second shock. From the second to third shock, the EPSP and IPSP reversals shifted an additional 3.0 ± 1.8 and 1.1 ± 0.7 mV, respectively. These shifts in reversal potential are manifested by the decreasing slopes of the fitted lines in the graphs where we plotted the PSP amplitudes as a function of membrane potential (—, 1st shock; - - -, 2nd and 3rd shocks; Fig. 9, *B,* IPSP, and *C,* EPSP).

Finally, we noted that the positive shift in IPSP reversal was accompanied by an increase in input resistance. The input resistance prior to and during the IPSPs was estimated by calculation of the slope resistance (the reciprocal of the slope

FIG. 5. Orthodromic responsiveness of entorhinal (*A, B,* and *D*) and perirhinal (*C*) neurons to LA and neocortical stimuli. ISI was 100 ms in all cases. *A*: the responsiveness of this entorhinal neuron to neocortical stimuli (*A1*) is not enhanced by conditioning LA shocks (*A2*). Same effect was seen at a lower stimulation intensity (not shown). *B*: rare case of entorhinal neuron with orthodromic responses to neocortical stimuli (35 superimposed sweeps). The responsiveness of this cell to the 2nd neocortical shock was reduced (from 14 to 3%). *C* and *D*: paired LA stimuli increase the orthodromic responsiveness of perirhinal (*C*) and entorhinal (*D*) neurons. *C* and *D* show the average field potential (*top*) and unit responses (superimposed sweeps) recorded simultaneously by the same microelectrode after differential digital filtering (field, 0.1–300 Hz; unit, 0.3–20 kHz). In addition, a peristimulus histogram is provided for each cell. Time scale in *C* also valid for *D.*

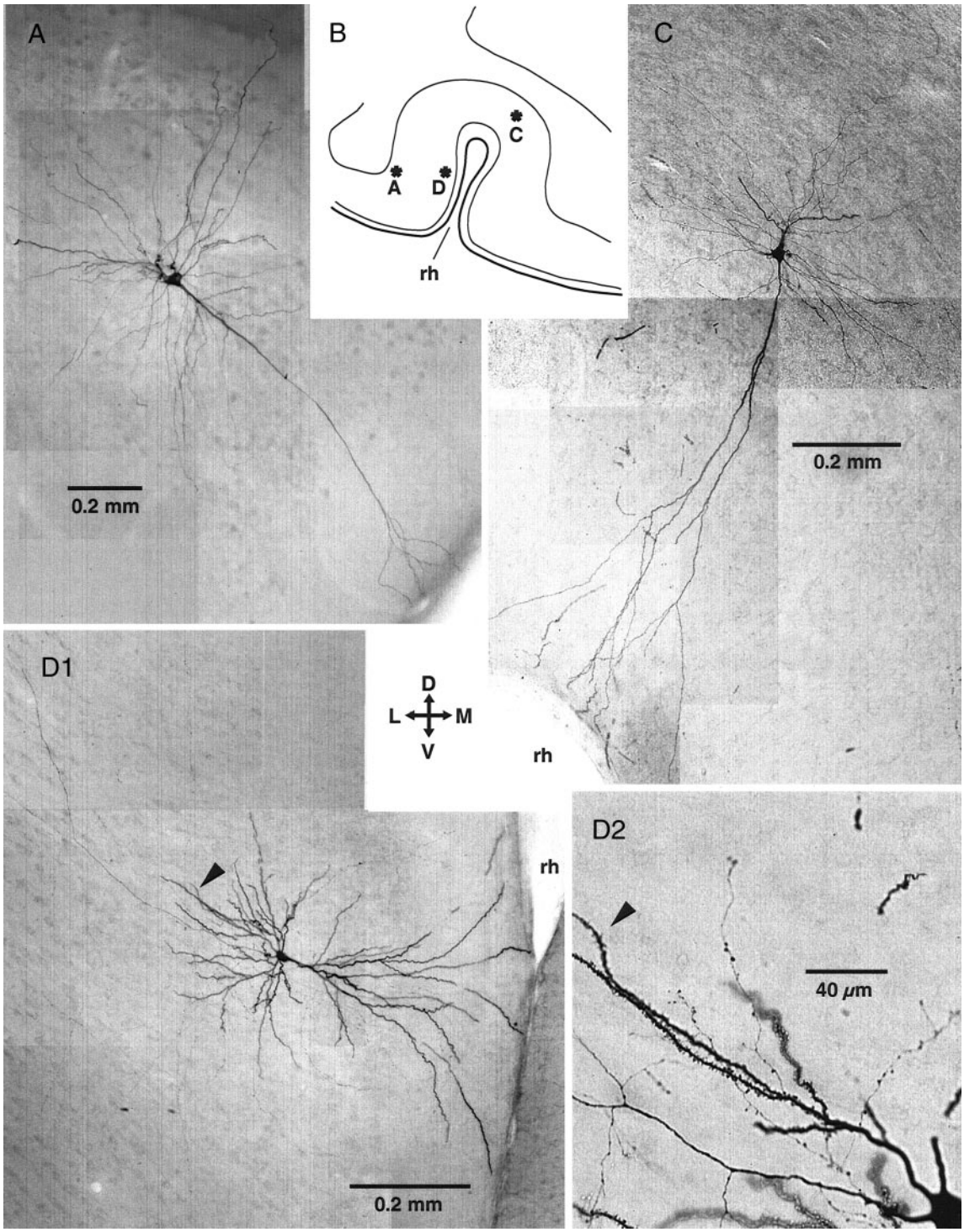

FIG. 6. Morphological identification of intracellularly recorded perirhinal neurons. *A, C,* and *D*: examples of perirhinal neurons morphologically identified with intracellular injection of neurobiotin. *B*: location of each cell. Orientation of the figures is indicated (+, D, dorsal; V, ventral; L, lateral; M, medial).

conductance) (Johnston and Wu 1995). Here the membrane potential was plotted against the DC current level before the first shock and at the IPSP peaks, and the slope of the fitted lines was used to estimate the input resistance of the cells at these various time points. From control values (29.0 ± 2.6 MΩ), the input resistance dropped 47.9 ± 9.5% at the first IPSP peak and then recovered 8.0 ± 2.4 and 3.2 ± 2.1% at the peak of the second and third IPSPs. These differences were statistically significant, paired *t*-test, $P < 0.05$). Note that in these analyses, measurements were obtained at fixed intervals between the stimulus artifact and the PSPs for all shocks. Several intervals were tested but qualitatively identical results were obtained.

When tested from rest with stimulus intensities that evoked spikes in 20–30% of trials at the first shock, most group I cells (10 of 12) showed an increased responsiveness to the second

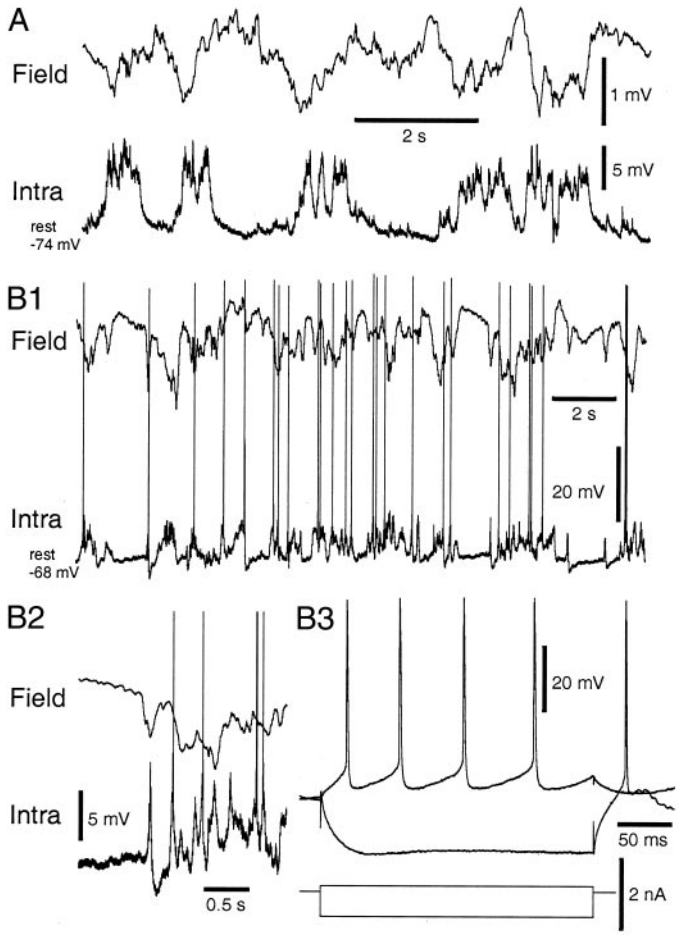

FIG. 7. Intracellular recordings of 2 different regular spiking perirhinal neurons recorded at rest (*A* and *B*). Spontaneous (*A* and *B, 1* and *2*) and current-evoked (*B3*) activity. Electroencephalographic (EEG) activity (field) recorded in the vicinity of recorded cells is depicted above the intracellular (intra) trace in *A* and *B, 1* and *2*.

shock. On average, the responsiveness to the second shock was 248 ± 42% of baseline.

Group II: cells with predominantly excitatory responses and PPF. In a second subset of perirhinal cells ($n = 8$), LA and neocortical stimuli evoked depolarizing responses with little overt inhibition (Fig. 10, *A* and *B*). Nevertheless, analysis of variations in response amplitudes as a function of the membrane potential usually (6 of 8 cells) revealed that they behaved similarly to the previous group of cells. That is, EPSP amplitudes increased from the first to the second and third shock (amplitude increase of 1.3 ± 0.5 and 2.2 ± 0.7 mV, respectively; paired *t*-test, $P < 0.05$), and this change was accompanied by a depolarization of their extrapolated reversal potential (positive shift of 10.7 ± 5.5 and 22.7 ± 13.7 mV, respectively, from a control value of −29.6 ± 8.4 mV; paired *t*-test, $P < 0.05$). When tested from rest with stimulus intensities that evoked spikes in 20–30% of trials at the first shock, these cells (6 of 6) showed an increase responsiveness to the second shock. On average, the responsiveness to the second shock was 185 ± 22% of baseline. In the remaining two cells, no shift in EPSP reversal potential was observed. In these cells, a simple summation of the EPSPs evoked by successive stimuli appear to underlie PPF (Fig. 10*B*).

Group III: cells with long-lasting inhibition resulting in PPD. In the rest of our sample ($n = 8$), both LA and cortical stimuli evoked small EPSPs followed by IPSPs that lasted longer than the ISI (100 ms; Fig. 10*C*) at all tested stimulation intensities. As a result, the second EPSP always occurred during the first IPSP, and no spike could be triggered. Analysis of responses to single shocks revealed that these IPSPs were composed of an early phase with a reversal potential of –74.3 ± 1.9 mV and a later one reversing in polarity at −84.3 ± 1.4 mV. In all these cells, repetitive stimulation at 10 Hz resulted in a reduced probability of orthodromic spiking to the second and third shocks, irrespective of the stimulation intensity.

Interestingly, the LA and neocortical-evoked responses of some group I (5 of 5 tested cells) and group II cells (4 of 6 tested cells) could be converted into a group III pattern by increasing the stimulation intensity. This phenomenon may explain why, in our extracellular recordings, many cells showing PPF at low stimulation intensities expressed PPD when the stimulating current was increased. An example of this is shown in Fig. 11 for a group II neuron. Note that at low stimulation intensities (100 μs, 0.5 mA; Fig. 11, thick line), neocortical stimuli evoked EPSPs with no overt inhibition. In contrast, when the stimulus duration was increased (300 μs, 0.5 mA, Fig. 11, thin line), the character of the response changed completely, the stimuli now evoking long-lasting IPSPs.

DISCUSSION

This study was undertaken to test whether LA inputs can facilitate the transfer of neocortical impulses across the rhinal cortices. We found that conditioning LA stimuli enhanced the amplitude of neocortically evoked field responses in both the peri- and entorhinal cortices, but that only in the former was this facilitation associated with increased orthodromic firing. Surprisingly, application of conditioning stimuli at the same or at a different neocortical site as the testing shock produced a similar facilitation of perirhinal field and unit responses. However, when the stimulation intensity was increased such that the first shock evoked orthodromic spikes in nearly all trials, the second shock rarely evoked spikes even though the field

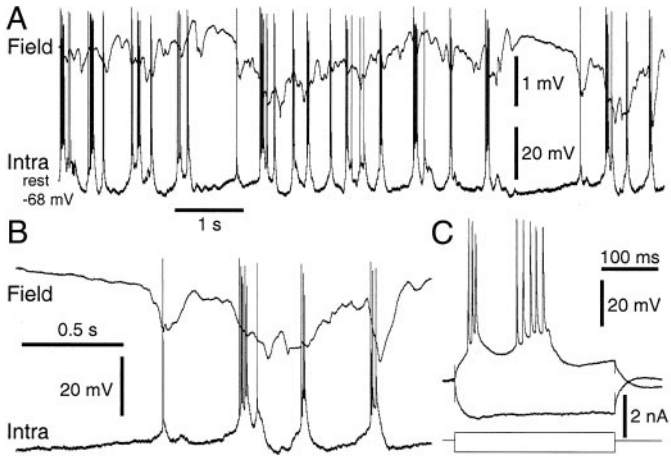

FIG. 8. Intracellular recording of the spontaneous (*A* and *B*) and current-evoked (*C*) activity of a bursting perirhinal neuron recorded at rest (*A* and B). EEG activity (field) recorded in the vicinity of recorded cell is depicted above the intracellular (intra) trace in *A* and *B*.

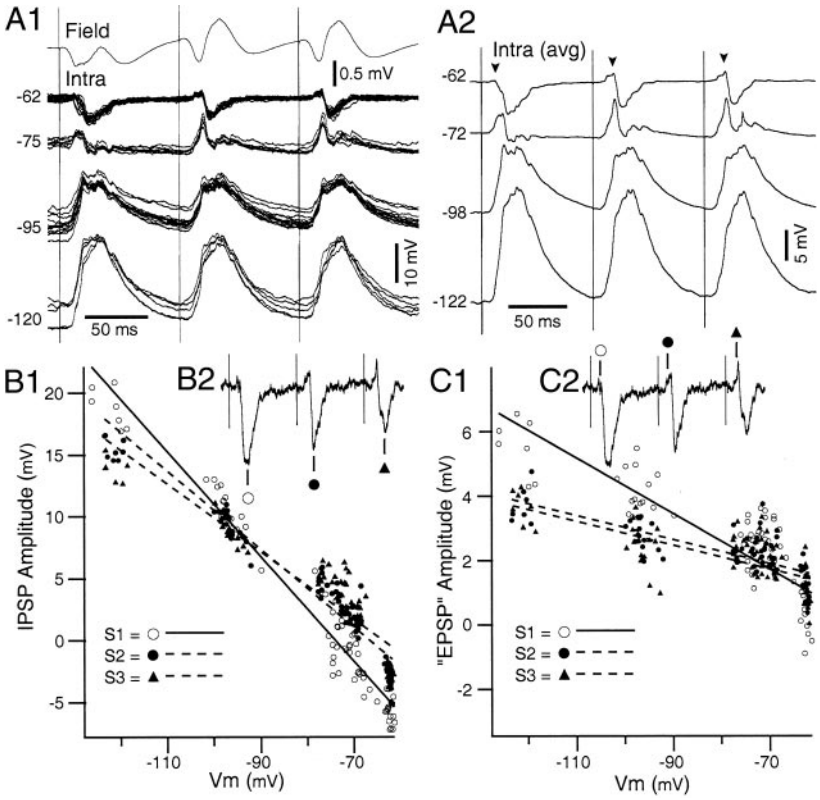

FIG. 9. In group I neurons, repetitive stimulation at 10 Hz produces a progressive increase in excitatory postsynaptic potential (EPSP) amplitude and reduction in inhibitory postsynaptic potential (IPSP) amplitude. *A*: responses evoked by repetitive LA stimuli at different membrane potentials as determined by intracellular current injection. *A1*, superimposed responses; *A2*, averaged traces. Note that many of the trials triggered spikes at depolarized levels; however, they were omitted from the figure and analyses. *B* and *C*: graphs plotting IPSP (*B*) and EPSP (*C*) amplitudes (*y* axis) as a function of membrane potential (*x* axis). In both graphs, linear fits were performed with the least-squares method (see legend in graphs). Amplitude measurements were performed on all available subthreshold trials at fixed intervals between the stimulus artifact and responses, as indicated in *B2* and *C2*, respectively. The resting potential was −82 mV in this cell.

response was still enhanced. Finally, intracellular recordings of perirhinal neurons revealed that the PPF seen at low stimulation intensities was associated with a rapid shift in the balance between inhibition and excitation whereas PPD prevailed in neurons where the first shock elicited long-lasting IPSPs. These results indicate that perirhinal neurons are subjected to strong feedforward and feedback inhibitory pressures, but that they can be modified dynamically depending on a complex interaction between stimulation frequency and intensity.

In the following account, we will discuss the significance of these observations in light of previous findings about the rhinal cortices and short-term synaptic plasticity.

Mechanisms of PPF and PPD in the perirhinal cortex

A large body of data indicates that synaptic efficacy can increase or decrease as a function of prior activity; such changes usually waning in seconds after a brief period of inactivity (reviewed in Zucker and Regher 2002). Depending on the types of synapses, facilitation, depression, or both can be observed (Thomson 2003).

In reduced preparations, where multisynaptic influences can be ruled out, PPF was shown to result from an increase in transmitter release probability due to residual Ca^{2+} in the presynaptic terminal (reviewed in Zucker and Regher 2002). Evidence for other contributing mechanisms was obtained, such as a depolarization-induced reduction in Ca^{2+} channel inhibition by G proteins (Brody and Yue 2000), but they vary between different types of synapses.

Similarly, multiple mechanisms of depression have been described. They include a reduction in the number of vesicles immediately available for release (von Gersdorff and Borst 2002), the release of modulators that act homo- or heterosynaptically (usually to inhibit release) (Miller 1998), and a variety of postsynaptic factors such as receptor desensitization (Jones and Westbrook 1996) and shifts in ionic gradients (Kaila 1994).

In an intact preparation, such as the one used in the present study, repetitive stimulation likely mobilized a number of the above mechanisms. Previous work in the cerebral cortex (reviewed in Thomson et al. 2002) indicates that synapses between pyramidal cells typically show frequency-dependent depression and PPD (Thomson and West 1993; Thomson et al. 1993a). In contrast, inputs from pyramidal cells onto many types of interneurons show facilitation and PPF (Markram et al. 1998; Thomson et al. 1993b; see Thomson et al. 2002). Finally, a majority of inputs from interneurons onto pyramidal cells show frequency-dependent depression (Gupta et al. 2000).

On the surface, the fact that synapses between pyramidal cells tend to depress, whereas pyramidal to interneuron synapses potentiate seems opposite to what we observed. We submit that the solution to this apparent contradiction resides in the frequency-dependent depression of synapses formed by interneurons onto pyramidal cells and the powerful intrinsic connections existing between pyramidal cells of the perirhinal cortex. Indeed, our results indicate that the EPSPs evoked by the first LA and neocortical shocks were countered by much inhibition. This was indicated by their relatively negative extrapolated reversal potential. Although the second shock likely caused release in fewer afferent fibers, this effect appears to have been compensated for by the reduced amount of GABA released by interneurons onto pyramidal cells. That this occurred in our experiments is suggested by the smaller decrease in input resistance associated to the second IPSPs and by the

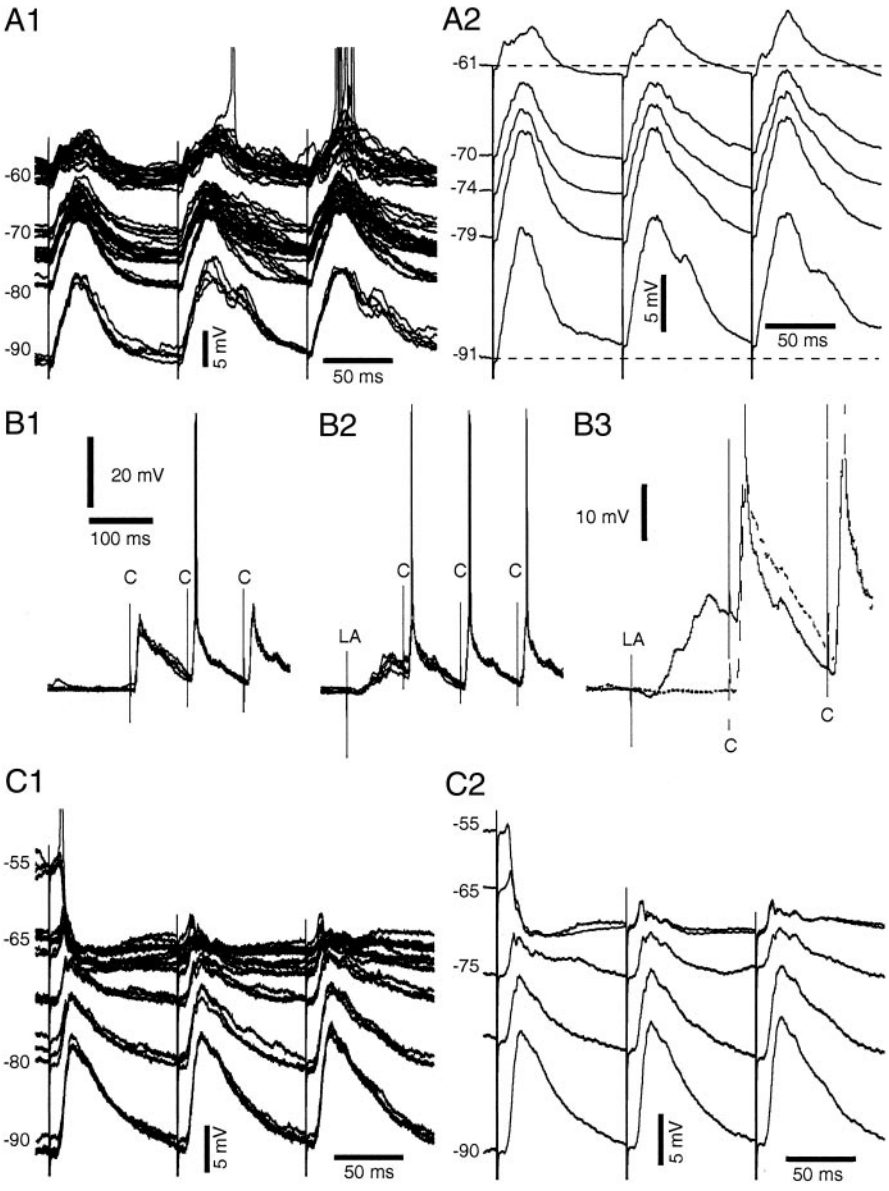

FIG. 10. Response patterns in group II (*A* and *B*) and III (*C*) neurons. Group II neurons show predominantly excitatory responses. *A*: responses evoked by repetitive neocortical stimuli at different membrane potentials as determined by intracellular current injection. *A1*, superimposed responses (spikes are truncated); *A2*, averaged traces (subthreshold trials only). Repetitive neocortical stimuli evoke multiphasic EPSPs with little overt inhibition. *B*: facilitation of suprathreshold orthodromic responses by summation of successive EPSPs. Repetitive neocortical stimuli (artifacts marked c) applied in isolation (*B1*) or preceded by a conditioning LA stimulus (marked LA) at rest. *B3*: expanded averages of the traces shown in *B, 1* and *2,* are superimposed (spikes are truncated). *C*: in group III neurons, shocks to the LA or neocortex evoke IPSPs that last longer than the ISI. This example shows response to neocortical stimuli at different membrane potentials as determined by intracellular current injection (spike truncated). *C1*, superimposed responses; *C2*, averaged traces. The resting potential was –79, −84, and –75 in *A–C,* respectively.

positive shift of the extrapolated reversal potential of the second EPSP. In addition, because perirhinal cells are interconnected, this effect is amplified; a proportion of pyramidal cells that were not recruited by the first shock are fired by the second, further exciting the recorded neuron.

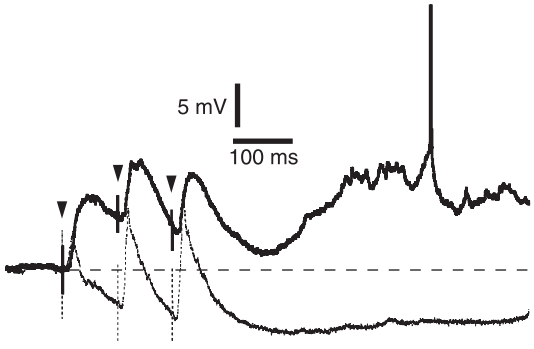

FIG. 11. Intensity-dependent response pattern. Response of the same cell to three neocortical shocks (0.5 mA) lasting either 100 μs (thick line) or 300 μs (thin line). Stimuli were applied at the same membrane potential (−65 mV), as determined by intracellular current injection (0.4 nA). The resting potential was –79 mV in this cell.

Postsynaptic factors may have contributed as well. Indeed, it is well known that during prolonged $GABA_A$ responses, the reversal potential ($E_{GABA\text{-}A}$) shifts positively (reviewed in Kaila 1994). In part, this change occurs because the chloride gradient collapses, revealing the contribution of a bicarbonate conductance to $GABA_A$ responses (Voipio and Kaila 2000). In a recent investigation of this phenomenon in pyramidal cells of the perirhinal cortex, it was estimated that $E_{GABA\text{-}A}$ shifted as much as 5 mV within 60 ms after the IPSP peak (Martina et al. 2001). This figure is consistent with the positive shift seen in the present study with repetitive stimulation.

In a proportion of cells, neocortical and LA shocks evoked prevalently inhibitory responses. In these cells, the IPSP evoked by the first shock lasted longer than the ISI. As a result, the second shock never fired these cells. Even though repetitive stimuli reduced the probability of orthodromic spiking in these cells, it is important to realize, however, that by hyperpolariz-

ing the cells, the IPSPs increased the inward current associated to the EPSPs, thereby contributing to enhance field responses.

In closing this section, it is important to mention that the response pattern displayed by a particular neuron presumably depends on the particular combination of synaptic inputs it receives and how they are recruited by our stimulating electrodes. The former is a rather fixed property of each cell, but the second depends on the stimulus intensity and the position of the stimulating electrodes.

Equivalence of LA and neocortical inputs in producing PPF

A surprising aspect of the present study was that LA and neocortical inputs had a similar effect on perirhinal neurons. Indeed, not only did electrical stimulation of these two sites evoke similar response patterns, but paired stimuli at one of the two sites evoked as much response facilitation as when the conditioning and testing shocks were applied at different sites. Although ultrastructural findings indicate that both inputs form a similar pattern of synaptic connections in the perirhinal cortex (Smith and Paré 1994; A. Pinto and D. Paré, unpublished observations), there are other possible explanations for these observations. First, it is possible that responses evoked from these two sites include a shared polysynaptic component. Second, because the LA and perirhinal cortex are reciprocally connected, it is likely that LA stimuli backfired perirhinal cells with branching axons to other perirhinal neurons. Thus it will be important to revisit the influence of LA inputs on perirhinal neurons, using chemical, rather than electrical stimuli.

Low probability perirhinal transfer of neocortical inputs to the entorhinal cortex

Much data suggest that perirhinal transfer of neocortical inputs to the entorhinal cortex is subjected to powerful inhibitory pressures. For instance, stimuli that evoke massive neuronal excitation in the perirhinal cortex generally do not fire principal entorhinal neurons in the whole guinea pig brain kept in vitro (Biella et al. 2001, 2003; De Curtis et al. 1999; Frederico et al. 1994). In addition, in vivo studies in anesthetized cats have shown that electrical stimuli delivered in the temporal neocortex activated $<2\%$ of tested entorhinal cells (Pelletier et al. 2004). This was not an artifact of the anesthesia because analysis of spontaneous activity in unanesthetized cats revealed that synchronized neuronal events occurring in relation to large-amplitude perirhinal EEG potentials also failed to excite entorhinal neurons (Pelletier et al. 2004).

The present study further strengthens the view that transmission between the peri- and entorhinal cortex is under tight inhibitory control. Although repetitive neocortical stimuli produced PPF in the perirhinal cortex, this increased perirhinal excitability did not augment the responsiveness of entorhinal neurons. This suggests that the increased magnitude of neocortically evoked field potentials seen in the entorhinal cortex after conditioning LA or neocortical stimuli was volume conducted from the perirhinal cortex or that the increased excitatory drive suggested by the field potential was insufficient to overcome the local inhibition. In this context, it should be mentioned that if neocortical stimuli produced feed-forward inhibition of entorhinal cells, this would increase the inward current associated to the EPSPs, resulting in an enhancement of field potential responses. Of course, it remains possible that entorhinal neurons display subthreshold EPSPs in response to neocortical stimuli (Biella et al. 2002). Such responses would be difficult to detect with extracellular recording techniques.

GRANTS

This work was supported by National Institute on Mental Health Grant R01MH-073610-01.

REFERENCES

Adolphs R, Cahill L, Schul R, and Babinsky R. Impaired declarative memory for emotional stimuli following bilateral amygdala damage in humans. *Learn Mem* 4: 291–300, 1997.

Biella GR, Uva L, and de Curtis M. Network activity evoked by neocortical stimulation in area 36 of the guinea pig perirhinal cortex. *J Neurophysiol* 86: 164–172, 2001.

Biella GR, Gnatkovsky V, Takashima I, Kajiwara R, Iijima T, and De Curtis M. Olfactory input to the parahippocampal region of the isolated guinea pig brain reveals weak entorhinal to perirhinal interactions. *Eur J Neurosci* 18: 95–101, 2003.

Biella GR, Uva L, and de Curtis M. Propagation of neuronal activity along the neocortical-perirhinal-entorhinal parthay in the guinea pig. *J Neurosci* 22: 9972–9979, 2002.

Brody DL and Yue DT. Relief of G-protein inhibition of calcium channels and short-term synaptic facilitation in cultured hippocampal neurons. *J Neurosci* 20: 889–898, 2000.

Buzsáki G. Two-stage model of memory trace formation: a role for noisy brain states. *Neuroscience* 31: 551–570, 1989.

Cahill L, Babinsky R, Markowitsch H, and McGaugh JL. The amygdala and emotional memory. *Nature* 377: 295–296, 1995.

Cahill L, Haier R, Fallon J, Alkire M, Tang C, Keator D, Wu J, and McGaugh JL. Amygdala activity at encoding correlated with long-term, free recall of emotional information. *Proc Natl Acad Sci USA* 93: 8016–8021, 1996.

Connors BW, Gutnick MJ, and Prince DA. Electrophysiological properties of neocortical neurons in vitro. *J Neurophysiol* 48: 1302–1320, 1982.

Davis M, Rainnie D, and Cassel M. Neurotransmission in the rat amygdala related to fear and anxiety. *Trends Neurosci* 17: 208–214, 1994.

De Curtis M, Takashima I, and Iijima T. Optical recording of cortical activity after in vitro perfusion of cerebral arteries with a voltage-sensitive dye. *Brain Res* 837: 314–319, 1999.

Frederico P and MacVicar BA. Imaging the induction and spread of seizure activity in the isolated brain of the guinea pig: the roles of GABA and glutamate receptors. *J Neurophysiol* 76: 3471–3492, 1994.

Gupta A, Wang Y, and Markram H. Organizing principles for a diversity of GABAergic interneurons and synapses in the neocortex. *Science* 287: 273–278, 2000.

Hamann SB, Ely TD, Grafton ST, and Kilts CD. Amygdala activity related to enhanced memory for pleasant and aversive stimuli. *Nat Neurosci* 2: 289–293, 1999.

Insausti R, Amaral DG, and Cowan WM. The entorhinal cortex of the monkey. II. Cortical afferents. *J Comp Neurol* 264: 356–395, 1987.

Johnston D and Wu SM-S. *Foundations of Cellular Physiology.* Cambridge, MA: MIT Press, 1995.

Jones MV and Westbrook GL. The importance of receptor desensitization on fast synaptic transmission. *Trends Neurosci* 19: 96–101, 1996.

Kaila K. Ionic basis of GABA-a receptor channel function in the nervous system. *Prog Neurobiol* 42: 489–535, 1994.

Kajiwara R, Takashima I, Mimura Y, and Iijima T. Amygdala input promotes spread of excitatory neural activity from perirhinal cortex to the entorhinal-hippocampal circuit. *J Neurophysiol* 89: 2176–2184, 2003.

Kapp BS, Whalen PJ, Supple WF, and Pascoe JP. Amygdaloid contributions to conditioned arousal and sensory information processing. In: *The Amygdala*, edited by Aggleton JP. New York: Wiley-Liss, 1992, p. 229–254.

Krettek JE and Price JL. Projections from the amygdaloid complex to the cerebral cortex and thalamus in the rat and cat. *J Comp Neurol* 172: 687–722, 1977a.

Krettek JE and Price JL. Projections from the amygdaloid complex and adjacent olfactory structures to the entorhinal cortex and to the subiculum in the rat and cat. *J Comp Neurol* 172: 723–752, 1977b.

LeDoux JE. Emotion circuits in the brain. *Annu Rev Neurosci* 23: 155–184, 2000.

Leung LS and Fu XW. Factors affecting paired-pulse facilitation in hippocampal CA1 neurons in vitro. *Brain Res* 650: 75–84, 1994.

Marder CP and Buonomano DV. Differential effects of short- and long-term potentiation on cell firing in the CA1 region of the hippocampus. *J Neurosci* 23: 112–121, 2003.

Markram H, Gupta A, Uziel A, Wang Y, and Tsodyks M. Information processing with frequency-dependent synaptic connections. *Neurobiol Learn Mem* 70: 101–112, 1998.

Martina M, Royer S, and Paré D. Cell-type-specific GABA responses and chloride homeostasis in the cortex and amygdala. *J Neurophysiol* 86: 2887–2895, 2001.

Miller RJ. Presynaptic receptors. *Annu Rev Pharmacol Toxicol* 38: 201–227, 1998.

Paré D, Smith Y, and Paré JF. Intra-amygdaloid projections of the basolateral and basomedial nuclei in the cat: *Phaseolus vulgaris*-leucoagglutinin anterograde tracing at the light and electron microscopic level. *Neuroscience* 69: 567–583, 1995.

Parker A and Gaffan D. Interaction of frontal and perirhinal cortices in visual object recognition memory in monkeys. *Eur J Neurosci* 10: 3044–3057, 1998.

Pelletier JG, Apergis J, and Paré D. Low probability transmission of neocortical and entorhinal impulses through the perirhinal cortex. *J Neurophysiol* 91: 2079–2089, 2004.

Pelletier JG and Paré D. Uniform range of conduction times from the lateral amygdala to distributed perirhinal sites. *J Neurophysiol* 87: 1213–1221, 2002.

Pennartz CM, Uylings HB, Barnes CA, and McNaughton BL. Memory reactivation and consolidation during sleep: from cellular mechanisms to human performance. *Prog Brain Res* 138: 143–166, 2002.

Pitkänen A, Pikkarainen M, Nurminen N, and Ylinen A. Reciprocal connections between the amygdala and the hippocampal formation, perirhinal cortex, and postrhinal cortex in rat. *Ann NY Acad Sci* 911: 369–391, 2000.

Richardson MP, Strange BA, and Dolan RJ. Encoding of emotional memories depends on amygdala and hippocampus and their interactions. *Nat Neurosci* 7: 278–285, 2004.

Room P and Groenewegen HJ. Connections of the parahippocampal cortex. I. Cortical afferents. *J Comp Neurol* 251: 415–450, 1986a.

Room P and Groenewegen HJ. Connections of the parahippocampal cortex in the cat. II. Subcortical afferents. *J Comp Neurol* 251: 451–473, 1986b.

Smith Y and Paré D. Intra-amygdaloid projections of the lateral nucleus in the cat: PHA-L anterograde labeling combined with post-embedding GABA and glutamate immunocytochemistry. *J Comp Neurol* 342: 232–248, 1994.

Suzuki WA. The anatomy, physiology, and functions of the perirhinal cortex. *Curr Opin Neurobiol* 6: 179–186, 1996.

Thomson AM. Presynaptic frequency- and pattern-dependent filtering. *J Comput Neurosci* 15: 159–202, 2003.

Thomson AM, Bannister AP, Mercer A, and Morris OT. Target and temporal pattern selection at neocortical synapses. *Philos Trans R Soc Lond* 357: 1781–1791, 2002.

Thomson AM, Deuchars J, and West DC. Large, deep layer pyramid-pyramid single axon EPSPs in slices of rat motor cortex display paired pulse and frequency-dependent depression, mediated presynaptically and self-facilitation, mediated postsynaptically. *J Neurophysiol* 70: 2354–2369, 1993a.

Thomson AM, Deuchars J, and West DC. Single axon excitatory postsynaptic potentials in neocortical interneurons exhibit pronounced paired pulse facilitation. *Neuroscience* 54: 347–360, 1993b.

Thomson AM and West DC. Fluctuations in pyramid-pyramid excitatory postsynaptic potentials modified by presynaptic firing pattern and postsynaptic membrane potential using paired intracellular recordings in rat neocortex. *Neuroscience* 54: 329–346, 1993.

Van Hoesen GW and Pandya DN. Some connections of the entorhinal (area 28) and perirhinal (area 35) cortices of the rhesus monkey. I. Temporal lobe afferents. *Brain Res* 95: 1–24, 1975.

Voipio J and Kaila K. GABAergic excitation and K^+-mediated volume transmission in the hippocampus. *Prog Brain Res* 125: 323–332, 2000.

von Gersdorff H, and Borst JG. Short-term plasticity at the calyx of held. *Nat Rev Neurosci* 3: 53–64, 2002.

Witter MP, Wouterlood FG, Naber PA, and Van Haeften T. Anatomical organization of the parahippocampal-hippocampal network. *Ann NY Acad Sci* 911: 1–24, 2000.

Zola-Morgan S, Squire LR, Alvarez-Royo P, and Clower RP. Independence of memory functions and emotional behavior: separate contributions of the hippocampal formation and the amygdala. *Hippocampus* 1: 207–220, 1991.

Zola-Morgan S, Squire LR, and Amaral DG. Lesions of the amygdala that spare adjacent cortical regions do not impair memory or exacerbate the impairment following lesions of the hippocampal formation. *J Neurosci* 9: 1922–1936, 1989.

Zucker RS and Regehr WG. Short-term synaptic plasticity. *Annu Rev Physiol* 64: 355–405, 2002.